https://doi.org/10.5194/egusphere-2024-2376
Preprint. Discussion started: 18 September 2024

Measurement report: The variation properties of aerosol hygroscopic growth related to chemical composition during new particle formation days in a coastal city of southeast China

Lingjun Li[1,2,3], Mengren Li[1,2,3*], Xiaolong Fan[1,2,3], Yuping Chen[1,2,3], Ziyi Lin[1,2,3], Anqi Hou[1,2], Siqing Zhang[1,2,3], Ronghua Zheng[1,2,3], Jinsheng Chen[1,2,3*]

[1] Institude of Urban Environment, Chinese Academy of Sciences, Xiamen 361021, China;
[2] Fujian Key Laboratory of Atmospheric Ozone Pollution Prevention, Institute of Urban Environment, Chinese Academy of Sciences, Xiamen 361021, China;
[3] College of Resources and Environment, University of Chinese Academy of Sciences, Beijing 100086, China

* Corresponding to: Jinsheng Chen (jschen@iue.ac.cn) and Mengren Li (mrli@iue.ac.cn)

Abstract. The scattering of solar radiation by aerosol is significantly affected by relative humidity (RH) due to the aerosol hygroscopicity. In order to better understand the characteristics of aerosol scattering hygroscopic growth and its influencing factors during new particle formation (NPF) days, we conducted the in-situ campaign from February to April 2022 in Xiamen, a coastal city in southeastern China. The aerosol scattering hygroscopic growth factor (f(RH)), commonly used to describe the aerosol hygroscopicity, varies greatly due to the influence of chemical composition and so on. In the relatively clean atmosphere of Xiamen, NPF occurs frequently and has an obvious effect on f(RH). In this study, we investigated the features and influencing factors of f(RH) in the NPF days. The research results emphasized that f(RH) differed significantly between NPF and Non-NPF days, mainly impacted by the aerosol chemical compositions, especially sulfate and nitrate. In the NPF days, sulfate was the dominant contributor to f(RH), distinguishing from the Non-NPF days. Aerosol hygroscopicity-chemical composition closure demonstrated that NH_4HSO_4 was the main source (30.78%) of the hygroscopicity parameter $\kappa_{f(RH)}$ when NPF events happened, while NH_4NO_3 played a dominant role in $\kappa_{f(RH)}$ (up to 35%) for Non-NPF days. Although the uncertainty of the organic aerosol (OA) to hygroscopicity might exist due to the varieties of chemical components and oxidation level, it was the crucial driving factor for the variation in aerosol hygroscopicity. The findings of this study would be helpful for the further understanding about the properties of aerosol hygroscopicity in the coastal area, as well as complementing the hygroscopic growth factors to the models of air quality and climate change.

1 Introduction

Atmospheric aerosols have direct and indirect effects on atmospheric visibility, the

https://doi.org/10.5194/egusphere-2024-2376
Preprint. Discussion started: 18 September 2024

earth-atmosphere radiation budget, clouds and precipitation, which in turn affect climate (Charlson et al., 1992); and these effects are strongly dependent on the hygroscopic properties of the ambient aerosol and the relative humidity (RH). The aerosol optical properties are key parameters for accurately estimating the direct radiative forcing caused by aerosols in climate models (IPCC, 2021). The aerosol hygroscopicity has a significant impact on the optical properties by altering particle size and refractive index, and ultimately on the climatic and environmental effects of aerosols (Covert et al., 1972;Tang, 1996;Malm and Day, 2001). Furthermore, aerosol hygroscopicity can profoundly affect atmospheric chemical processes (Wu et al., 2018) and air quality (Liu et al., 2020a).

Aerosol hygroscopic growth become the main factors affecting the aerosol optical properties at high ambient humidity due to the enhanced aerosol hygroscopicity and increased RH (Jin et al., 2022). The aerosol scattering hygroscopic growth factor (*f*(RH)) is defined as the ratio of aerosol scattering coefficient at an elevated RH level (σ_{sp}(RH, λ)) to that under dry condition (σ_{sp}(RH_{dry}, λ)) (usually RH < 40 %) at a given wavelength. The scattering enhancement owing to hygroscopic growth strongly depends on the source of the aerosol, which varies in chemical composition (Yan et al., 2009;Sheridan et al., 2002;Fierz-Schmidhauser et al., 2010a;Kotchenruther and Hobbs, 1998). For example, marine aerosols tends to have higher *f*(RH) than urban or continental aerosols, and their *f*(RH) decreases under strong anthropogenic influence (Zieger et al., 2010;Yan et al., 2009;Sheridan et al., 2001). Mineral dust and newly emitted biomass combustion aerosols have significantly lower *f*(RH) values (Sheridan et al., 2002;Pan et al., 2009;Fierz-Schmidhauser et al., 2010a). Hydrophilic species such as secondary inorganic components, sea salts, and water-soluble organics in the aerosol are the main contributors to the hygroscopic growth, while black carbon and some organic carbons are the major proportion of the hydrophobic species. Thus, discrepancies in the chemical composition of the aerosol, the fraction of soluble and insoluble chemical components, i.e., lead to variations of *f*(RH) (Malm et al., 2005;Zieger et al., 2014;Zhang et al., 2015). Additionally, particle number size distribution (PNSD) is another factor affecting *f*(RH). For a fixed chemical composition, *f*(RH) decreases with increasing particle size (Fierz-Schmidhauser et al., 2010b). Noted that the aerosol chemical compositions and the particle sizes have a combined impact on *f*(RH) in the atmospheric environment, as the two are closely related (Wu et al., 2017).

The observation site is situated in Xiamen, a fast-urbanization coastal city in southeastern China, at the junction of land and sea. As a result of massive population growth and rapid economic development, its atmospheric environment is subjected to complex pollution situations, such as the increased atmospheric oxidation (Liu et al., 2022)and relative high nitrogen oxide pollution (Chen et al., 2023) despite the aerosol concentrations are generally at a relative low level. On the other hand, it is located at a subtropical city with a relative high air temperatures and high RH. High RH not only directly increases light scattering, leading to the decline of visibility (Won et al., 2021),

https://doi.org/10.5194/egusphere-2024-2376
Preprint. Discussion started: 18 September 2024

but also affects the aerosol chemical processes involved in the particle formation(Sun et al., 2013;Chen et al., 2021). New particle formation (NPF) events occur frequently in this coastal city in southeast China with relative clean air quality (Wang et al., 2022). NPF is a process that low-volatile compounds emitted from natural or anthropogenic sources form into thermodynamically stable molecular clusters and grow into larger particles via condensation or collision with other vapours or particles (Holmes, 2007). When NPF occurs, both the PNSD and the chemical composition of the aerosol undergo significant changes, which have a remarkable influence on the aerosol hygroscopicity and *f*(RH). Previous studies of *f*(RH) had been conducted mainly in the megacity agglomerations such as North China Plain, Yangtze River Delta and Pearl River Delta (Liu et al., 2012;Xia et al., 2019;Ding et al., 2021;Jin et al., 2022), while limited attention had been paid to the southeast coastal areas with relative low level of particle and high RH. Meanwhile, these studies have focused more on the effect of aerosol chemical composition on *f*(RH) (Titos et al., 2014;Li et al., 2021;Wang et al., 2021;Jin et al., 2022), however, the exploration to the relationship between *f*(RH) and NPF is quite few in China, especially during NPF period.

In order to investigate the characteristics of *f*(RH) and its influencing factors during the NPF days, this study utilized a high-resolution, humidified nephelometer system combined with the PNSD instruments to observe *f*(RH) for RH ranging from 40% to 91% in urban Xiamen. Other aerosol chemical and physical properties were also synchronously measured. Differences and variations in *f*(RH) between NPF and Non-NPF days were explored and the effect of aerosol chemical compositions on *f*(RH) were also discussed. The research was expected to characterize the properties of aerosol hygroscopicity during the NPF and Non-NPF days in coastal area with relative low level of particle and high RH, and provide references to the model improvement for air quality and climate change.

2 Instruments and methods

2.1 Observation site

The enhanced observations were carried out at the Institute of Urban Environment of the Chinese Academy of Sciences in Xiamen (IUE, CAS), which is situated on the west coast of the Taiwan Strait. The observation station (118°03′E, 24°36′N) was located on the roof of an 80m-heigh building, a typical urban site surrounded by two main trunk roads (Jimei main road and Haixiang express road), shopping malls, educational institutions, and residential areas, and there was no apparent industrial emission sources nearby. Thus, the collected data can accurately represent the average air quality levels in the urban area of Xiamen. The observations were conducted consecutively from the 1st February to the 30th April 2022.

2.2 Observation instruments

The *f*(RH) values were obtained using a multi-band dual-nephelometer system (PB-FRH100, BMET, China) comprising a nephelometer for aerosol scattering coefficients under dry conditions and another nephelometer for humidified aerosols.

https://doi.org/10.5194/egusphere-2024-2376
Preprint. Discussion started: 18 September 2024

The airflow initially entered through the $PM_{2.5}$ inlet and then passed through two tandem Nafion dryers which could decrease the RH of the airflow to less than 30%. After this, the airflow was divided into two routes, one was directed straight into the nephelometer, while the other was humidified via a Gore-Tex tube set in a stainless steel tube before flowing into the nephelometer. The space between these two tubes contained circulating water, which was heated by a water bath. The scattering coefficients of dry and humidified $PM_{2.5}$ were measured at three wavelengths (450, 525 and 635 nm) using two nephelometer. The detailed principles and operation of the system has been described in previous studies (Liu and Zhao, 2016;Kuang et al., 2017;Zhao et al., 2019). This study set the minimum and maximum RH at 40% and 91%, respectively, with a 45-minute cycle for humidification.

An integrating nephelometer (Aurora-3000, Ecotech, Australia) was used to simultaneously and continuously measure the 5-min average σ_{sp} at the same three wavelengths, and the σ_{sp} at 525 nm was consistent with the objectives of this study. A Scanning Mobility Particle Sizer (SMPS, model 3938 L50, TSI Inc., USA), integrated with a Differential Mobility Analyzer (DMA, model 3082, TSI Inc., USA), a butanol-based Condensation Particle Counter (CPC, model 3750, TSI Inc., USA) and an aerosol neutralizer, were used to continuously measure the PNSD in the range of 7-300 nm over a 5-minute scanning interval during the measurement. The hourly chemical composition of aerosol, including sulfate (SO_4^{2-}), nitrate (NO_3^-), ammonium (NH_4^+), chloride (Cl^-) and organic matter (OM), was measured by a high-resolution Aerodyne Aerosol Chemical Speciation Monitor (ACSM). An AE-31 aethalometer (Magee Scientific, USA) was used to measure the balck carbon (BC) aerosol concentrations. Hourly mass concentrations of $PM_{2.5}$ were measured by a Tapered Element Oscillating Microbalance (TEOM1405, Thermo Scientific Corp., USA). Ambient meteorological parameters, including air temperature (T), RH, wind speed (WS) and wind direction (WD), were continuously monitored by an ultrasonic weather station instrument (150WX, Airmar, USA).

2.3 Identification and classification of new particle formation

The NPF process involves nucleating and growing. The particles nucleated at a critical size of approximately 1.5 ± 0.4 nm (Kulmala et al., 2012) and then could grow into larger particles. During the sampling period, 85 days were available for NPF classification analysis. The particles were divided into three modes: nucleation mode (< 25 nm), Aitken mode (25-100 nm) and accumulation mode (> 100 nm) in this study (Kalkavouras et al., 2021;Shen et al., 2022;Wang et al., 2022). To identify NPF events, the visual analysis of PNSD data described by Dal Maso et al. (2005) was used. If a new particle mode is observed in the nucleation mode within a few hours and the mode shows clear signs of growth, characterized by a distinct “banana” shape in the time series of PNSD, then the day can be classified as an NPF event day. With the exception of NPF days, all other days are classified as Non-NPF days or Undefinded days. Non-NPF days are confirmed when there is clearly no evidence of NPF or when the above criteria are not met. Besides, days that can not fulfil the criteria to be identified as NPF

https://doi.org/10.5194/egusphere-2024-2376
Preprint. Discussion started: 18 September 2024

or Non-NPF days were classified as Undefined days, and they are characterised by the presence of some particles in the nucleation mode with no visible signs of growth, or by the observation of growth not in the nucleation mode.

2.4 Data processing

The scattering Ångström exponent (α) indicates the wavelength dependence of aerosol scattering, and the parameters related to aerosol size are relatively low for large particles and relatively high for small particles(Guan et al., 2021). It is expressed as follows:

$$\alpha = \frac{\log(\sigma_{sp,\lambda_1}) - \log(\sigma_{sp,\lambda_2})}{\log(\lambda_1) - \log(\lambda_2)} \quad (1)$$

Where, λ_1=450 nm and λ_2=635 nm in this study.

The fitting parameter γ is defined as $\gamma = \ln f(RH)/\ln((100/RH_{ref})/(100-RH))$(Quinn et al., 2005;Zhang et al., 2015). Here γ was based on RH_{ref} = 40 % and RH = 80 %. The relative quantity of OM and inorganic matters can be expressed as $F_o = OM/(OM + C_i)$, where C_i is the mass concentration of SNA. We chose NO_3^-, SO_4^{2-}, NO_3^- + SO_4^{2-} and NO_3^- + SO_4^{2-} + NH_4^+ as different SNA constitute in this study, respectively.

The overall hygroscopicity parameter $\kappa_{f(RH)}$ can be obtained from the measured f(RH) by summing the simultaneously measured PNSD and mass concentrations of BC, as proposed by Chen et al. (2014)and interpreted and refined by Kuang et al. (2020). The detailed calculation procedure of this method is shown in Kuang et al. (2017).

For the calculation of the hygroscopicity parameter κ based on the measured aerosol chemical-composition data, we used the mass concentrations of OA, SO_4^{2-}, NO_3^-, NH_4^+ and Cl^- provided by ACSM. In this study, a simplified ion pairing scheme proposed by Gysel et al. (2007) was used to obtain the concentrations of AN, AS, ABS, and AC by turning mass concentrations of ions into mass concentrations of the corresponding inorganic salts. The κ values and densities of these salts are shown in Table S1 (Liu et al., 2014;Wu et al., 2016;Kuang et al., 2020). The simple mixing rule, called Zdanovsky-Stokes-Robinson (ZSR), is commonly used in κ_{chem} calculations, therefore, the κ_{chem} of this study can be calculated on the basis of chemical volume fractions ε_i (Petters and Kreidenweis, 2007) (see Text S1 for a detailed process).

3 Results and discussion

3.1 Overview of f(RH) and derived aerosol variables observations

The typical levels of light scattering coefficients (σ_{sp}), f(RH) values at RH = 80% (f(80%)), scattering Ångström exponents (α), $PM_{2.5}$ mass concentrations, and ambient RH from February to April 2022 were displayed in Figure S1. To evaluate the aerosol hygroscopicity conveniently, f(80%) was often employed (Xia et al., 2023;Xia et al., 2019;Zhao et al., 2019;Wu et al., 2017). The scattering hygroscopic growth factor f(80%) ranged from 1.00 to 2.48, with an average factor of 1.44 ± 0.15 during the whole campaign. The mean concentration of $PM_{2.5}$ was 24.79 ± 17.74 μg m^{-3}, suggested the $PM_{2.5}$ pollution was relative low in Xiamen according to the air quality index (AQI) grading standard of China. During the period of observation, the hourly mean σ_{sp}

https://doi.org/10.5194/egusphere-2024-2376
Preprint. Discussion started: 18 September 2024

measured under dry conditions varied from 1.15 to 662.57 Mm^{-1}, with a mean and standard deviation of 135.50 ± 108.78 Mm^{-1}, and its maximum occurred at the peak of $PM_{2.5}$ concentrations. The α was usually considered as an indicator of particle size, which was high when $PM_{2.5}$ level was low, indicating that there were more fine particles existed in $PM_{2.5}$ with low concentration. At the same time, the variation trend of *f*(80%) was similar to that of α. Ambient RH fluctuated considerably and was generally at a high level. The wind direction was more evenly distributed, and the wind speed was relatively stable, concentrated in 1-3 m/s. The comparison presented in Table S2 implied that *f*(RH) varied widely across different regions, with consistently higher values observed in Europe compared to China. The differences between *f*(RH) in this study and in other regions of China were smaller than those compared with outside of China.

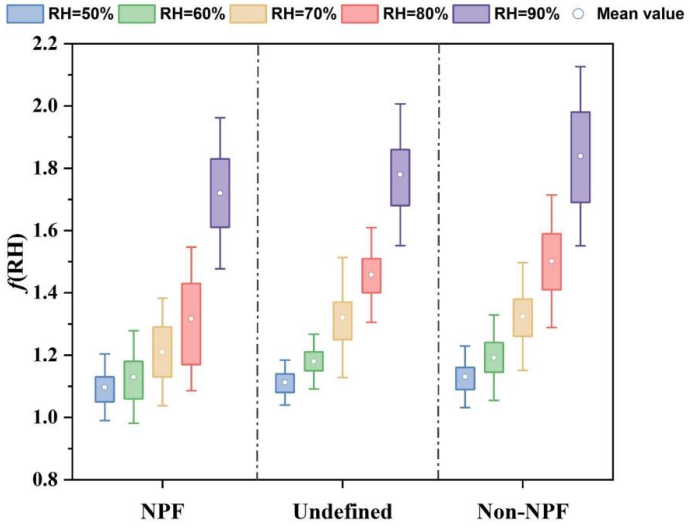

Figure 1. The *f*(RH) measured for a given RH in different days. The *f*(RH) values at RH=50%, 60%, 70%, 80%, and 90% were counted for the three types of days NPF, Undefined, and Non-NPF, respectively. Different colours represent different RH.

The entire campaign was devided into three type of days, NPF, Undefined, and Non-NPF, based on the above classification method. The PNSD spectrum and number concentration of the example NPF and Non-NPF days from February to April 2022 are shown in Figure S2 and Text S2. 11 NPF days were identified, representing approximately 12.94% of all observed days. In addition, we categorized 18 days as Non-NPF days, and the remaining days as Undefinded. The statistical analysis of particle number concentrations in different days during the observation period was summarized in Table S3. The mean number concentration of nucleation, aitken and accumulation mode was 1.66×10^3 cm^{-3}, 3.80×10^3 cm^{-3} and 8.59×10^2 cm^{-3} in NPF

https://doi.org/10.5194/egusphere-2024-2376
Preprint. Discussion started: 18 September 2024

days, contributing 26.25%, 60.14% and 13.61% to total concentration, respectively. The majority of particle number concentrations were comprised of nucleation and aitken mode particles. Figure 1 explores the variations of *f*(RH) with RH growth in different days. Firstly, *f*(RH) emerged an approximately exponential rise as RH increasing, with a significant growth when the RH ranged from 80% to 90%, the interval of which was the most beneficial to the aerosol scattering hygroscopic growth. However, Zhao et al. (2019) found a prominent difference in the aerosol hygroscopicity as RH beyond 90%, and the aerosol hygroscopicity in this humidity range was lower than that when RH was below 90%. Secondly, the characteristics of *f*(RH) was distinct among the different days, although the discrepancies in statistical parameters, such as the mean and median values of *f*(RH) were minor. When RH was below 80%, *f*(RH) was significantly lower during NPF days compared to Non-NPF and Undefined days. The *f*(RH) growth of NPF days was greater than those of the other two sorts of days for RH between 80 and 90 %, and vice versa for RH below 80%. Such a growth pattern caused the *f*(RH) of the NPF days reaching a level equivalent to that of the other days as the RH rose to 90%. Moreover, the fluctuations of *f*(RH) were larger in the NPF days than in the other two sorts of days, indicating *f*(RH) in NPF days had a greater dispersion. These results might be related to the dramatic increase in particle number concentrations and variations in chemical composition during the NPF days.

The following discussion will focus on the differences in the aerosol scattering hygroscopic growth and the aerosol hygroscopicity between NPF and Non-NPF. As Undefined days are in a transitional state, they do not accurately reflect the characteristics of the NPF.

3.2 Parameterization of the *f*(RH)

To better characterize the dependence of *f*(RH) on RH, many different empirical expressions have been applied in previous studies to fit the measurements of *f*(RH) (Kotchenruther et al., 1999;Kotchenruther and Hobbs, 1998;Gasso et al., 2000;Carrico et al., 2003;Pan et al., 2009;Zieger et al., 2014;Yu et al., 2018). We fitted four commonly-used empirical equations to the *f*(RH) values, and compared the results to find that Eq. (1) (Chen et al., 2014) was the most suitable for describing the enhanced scattering caused by the monotonic hygroscopic growth (see Figure S3 and Text S3 for a detailed comparison).

$$f(\mathrm{RH}) = a\left(1 - \frac{RH}{100}\right)^{-b\left(\frac{\mathrm{RH}}{100}\right)} \quad (2)$$

where *a* is a coefficient that reflects the level of *f*(RH) values, and *b* is the parameter for the magnitude of scattering enhancement unaffected by RH that quantifies aerosol hygroscopicity to some extent. Higher *f*(RH) is related to higher “a” and “b” values.

The fitted *f*(RH) curves between NPF and Non-NPF days over the entire observation period are presented in Figure 2. For these days, Eq.(2) was a difference in the fitting results, with fitting degrees being better in Non-NPF days and relatively worse in NPF days. This reflected that *f*(RH) was influenced by more complex factors

https://doi.org/10.5194/egusphere-2024-2376
Preprint. Discussion started: 18 September 2024

during NPF period. The fitted *f*(RH) curve shown in Figure 2(a) is apparently below that shown in Figure 2(b). Similarly, both the observed *f*(80%) and the simulated *f*(80%) in the NPF days were lower compared to those in the Non-NPF days. The *b* was lower for the NPF days, indicating that the aerosol hygroscopicity of the NPF days was weaker than those of Non-NPF days. In this work, *b* was lower than that in the study done by Zhao et al. (2019), but slightly higher than the findings of Chen et al. (2014) (Table S4), even though both of their studies were conducted in the North China Plain (NCP), where $PM_{2.5}$ concentrations and *f*(RH) were higher than those in Xiamen. Due to the proximity of *a*, a smaller *b* value resulted in the *f*(RH) being lower in this study compared to those in the NCP. It should be noted that the aerosol scattering hygroscopic growth does not necessarily diminish completely even in atmospheric environments with relatively low levels of particle pollution. This also shows that aerosol scattering hygroscopic growth is mainly controlled by the aerosol properties, such as aerosol chemical composition, etc., which is strongly related to the particle formation mechanism and the source of fine particles (Li et al., 2021;Chen et al., 2022a).

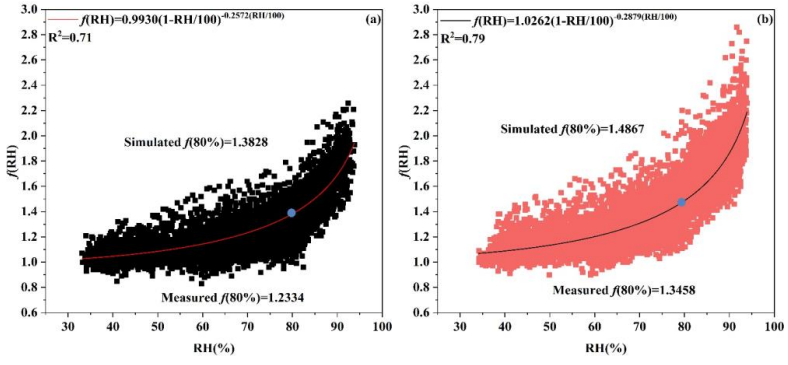

Figure 2. The *f*(RH) curves fitted by Eq.(1) between NPF and Non-NPF days. (a) belongs to NPF days, (b) belongs to Non-NPF days. Red and black lines are the curves fitted by Eq. (1), and blue dots represent the simulated values of *f*(80%).

3.3 Distribution characteristics of *f*(RH) and aerosol chemical compositions

Aerosol chemical compositions play a vital role in the aerosol hygroscopic growth. The mass concentration of the chemical components in NR-PM_1 (nonrefractory submicron particles), including SO_4^{2-}, NO_3^-, NH_4^+, Cl^- and OM, and BC in aerosols were displayed in Table S5. SO_4^{2-}, NO_3^- and NH_4^+ (SNA) constituted the majority of the inorganic ions, which were converted from gaseous precursors by complex chemical processes in the atmosphere. In the last decade, the concentrations of all SNA in Xiamen have significantly decreased (Deng et al., 2016). The decline ratio in sulfate concentration reached 84.0%, indicating the effectiveness of sulfate control measures in recent years. However, in contrast to the winter in 2013, the proportion of nitrate was greater than that of sulfate in this study, suggesting that nitrate pollution has become more prominent in recent years. The concentration of OM decreased in comparison to

https://doi.org/10.5194/egusphere-2024-2376
Preprint. Discussion started: 18 September 2024

the previous study, while its proportion in aerosol remained unchanged (Chen et al., 2022b). Additionally, BC is regarded as hydrophobic species (Zieger et al., 2014).

The diurnal variation of *f*(80%) and chemical mass fractions are displayed in Figure 3. The diurnal variation of *f*(RH) was significantly related to the mass fraction of chemical components in particle. NPF days had an obvious lower values of *f*(80%) compared with the other event. The mass concentration of PM_1 in the Non-NPF days (12.00 μg m^{-3}) was slightly lower than those in the NPF days (12.40 μg m^{-3}). The mass fraction of OM in the aerosol was higher during the NPF period than during the Non-NPF period, and *f*(80%) in the NPF period was smaller than that in the Non-NPF period. The increasing fraction of OM might be attributed to the emissions from heavy truck in the major roads near the observation site, which had a weaker impact on the aerosol hygroscopic growth than the SNA.

The *f*(80%) showed the same pattern as the mass fraction of SNA, especially for nitrate, and the amount of nitrate was significantly low during NPF period. The mass fraction of sulfate was much higher than that of nitrate for NPF compared to Non-NPF, which was accounted for the sulfuric acid was involved and played an active role during the NPF period (Sipilä et al., 2010;Wang et al., 2022). Noted that the lower *f*(80%) in NPF period was probably attributed to the low mass fraction of nitrate and high mass fraction of sulfate in SNA. Chen et al. (2022a) reported that aerosol hygroscopic growth in Shanghai and Guangzhou during NPF days were lower than those during Non-NPF days, which were consistent with the results of this study, but the opposite pattern occurred in the NCP. This illuminates that fewer hygroscopic particles were born during the NPF event in Xiamen. The study by Liu et al. (2021) also found that the hygroscopicity of 40 nm organic aerosol (OA) was significantly enhanced during NPF days in urban Beijing, which could be accounted for contribution of different precursors during the NPF process. In addition, when particle formation occurs in NPF days, the condensation of large quantities of sulfuric acid and organic vapours onto the pre-existing particles, resulting the conversion of mixed state on the surface of particles from external mixture to internal mixture and alteration of the optical and chemical properties of particles, which in turn would change the aerosol scattering hygroscopicity growth (Wu et al., 2016).

The sulfur/nitrogen oxidation ratios (SOR/NOR) used to assess the extent of secondary sulphate and nitrate formation are shown in Figure 4, which were calculated from the formulas of NOR=$[NO_3^-]/([NO_3^-]+[NO_2])$ and SOR=$[SO_4^{2-}]/([SO_4^{2-}]+[SO_2])$, respectively (Liu et al., 2020b). The levels of SOR and NOR were subjected to the regulation by photochemical reactions, exhibiting an increase during daytime. Moreover, the variations in SOR/NOR levels and *f*(80%) across NPF days were found to be coincident, as SOR/NOR levels droped down, particularly for NOR, *f*(80%) also displayed a low level. We assume that nitrate was essential for the aerosol scattering hygroscopic growth, as confirmed by a significant decline in *f*(RH) when both nitrate content and NOR were low, especially during NPF days. The sharp rise in NOR in the afternoon during the NPF days resulted in an significant increase in the relative amount

https://doi.org/10.5194/egusphere-2024-2376
Preprint. Discussion started: 18 September 2024

of nitrate in the aerosol and *f*(80%), indicating the rapid response of the aerosol hygroscopic growth to nitrate, which can be interpreted as a stronger hygroscopicity of nitrate compared to sulfate. In Non-NPF days, SOR and NOR were enhanced, which might be resulted from the aqueous phase reaction at relatively high RH (Sun et al., 2013;Ge et al., 2012).

In brief, the influence of SNA on *f*(RH), particularly nitrate, is significant. Sulfate dominated the SNA during the NPF days, characterized by weaker aerosol hygroscopic growth compared to Non-NPF days, indicating the intricate formation mechanisms for new particles and local sources of precursors on aerosol hygroscopic growth.

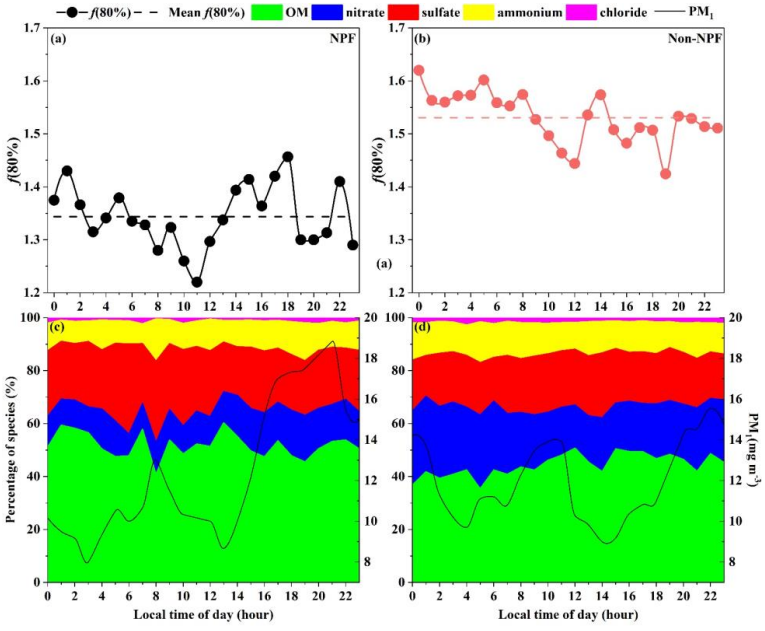

Figure 3. Diurnal variations of *f*(80%) and aerosol chemical mass fractions between NPF and Non-NPF days. (a) and (c) belong to NPF days, (b) and (d) Non-NPF days. These chemical compositions include OM, NO_3^-, SO_4^{2-}, NH_4^+, Cl^-. Solid lines are the mass concentrations of PM_1, dashed lines are the mean value of *f*(80%).

https://doi.org/10.5194/egusphere-2024-2376
Preprint. Discussion started: 18 September 2024

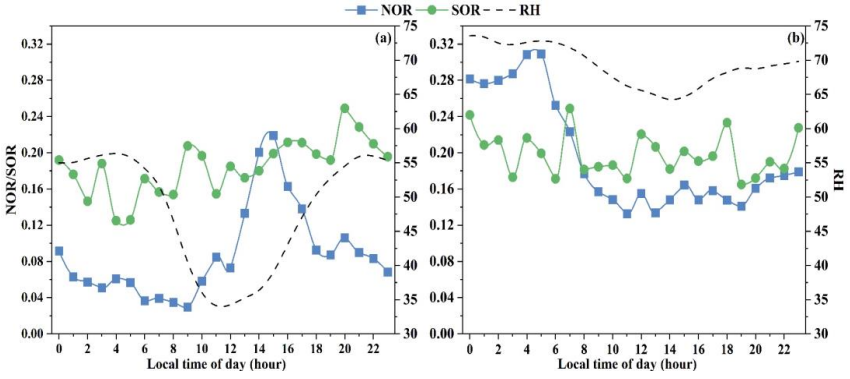

Figure 4. Diurnal variations of NOR, SOR and RH between NPF and Non-NPF days. (a) belongs to NPF days, (b) belongs to Non-NPF days. Blue represents NOR, green represents SOR, dashed lines are RH.

3.4 Relationships between *f*(RH) and aerosol chemical compositions

Figure 5 and Figure 6 exhibits *f*(80%) as a function of the mass fractions of SNA and OM between NPF and Non-NPF days, revealing the effect of chemical compositions on the aerosol scattering hygroscopic growth. The SNA fraction showed a positive correlation with *f*(80%) as a result of its high hygroscopicity, whereas the OM fraction demonstrated a negative correlation with *f*(80%) due to its relative lower hygroscopicity compared to SNA, in line with findings from previous studies (Zhang et al., 2015;Wu et al., 2017;Ren et al., 2021;Zieger et al., 2014). The magnitude of R for the linear regression was higher during the NPF period compared to the Non-NPF period, illuminating a stronger correlation between *f*(80%) and the mass fraction of SNA or OM specifically during NPF days. The proportion of aerosol chemical compositions remained relatively stable during the Non-NPF days, which could be accounted for the limited correlation between *f*(80%) and their mass fractions during this period. Comparing Figure 5a, 5b with Figure 6a, 6b, there was a stronger relationship between mass fraction of sulfate and *f*(80%) in NPF days. Conversely, a stronger association of *f*(80%) with nitrate was observed in Non-NPF days. This indicated that sulfate played a major role in influencing the aerosol hygroscopicity enhancement during NPF period, while nitrate was the primary contributor for Non-NPF days. This phenomenon could be explained by that the mass fraction of sulfate in the SNA was highest when the NPF event occurred, yet the differences between the mass fractions of sulfate and nitrate were slight in Non-NPF days. The role of nitrate in the aerosol hygroscopic properties will be discussed in the following paragraphs.

https://doi.org/10.5194/egusphere-2024-2376
Preprint. Discussion started: 18 September 2024

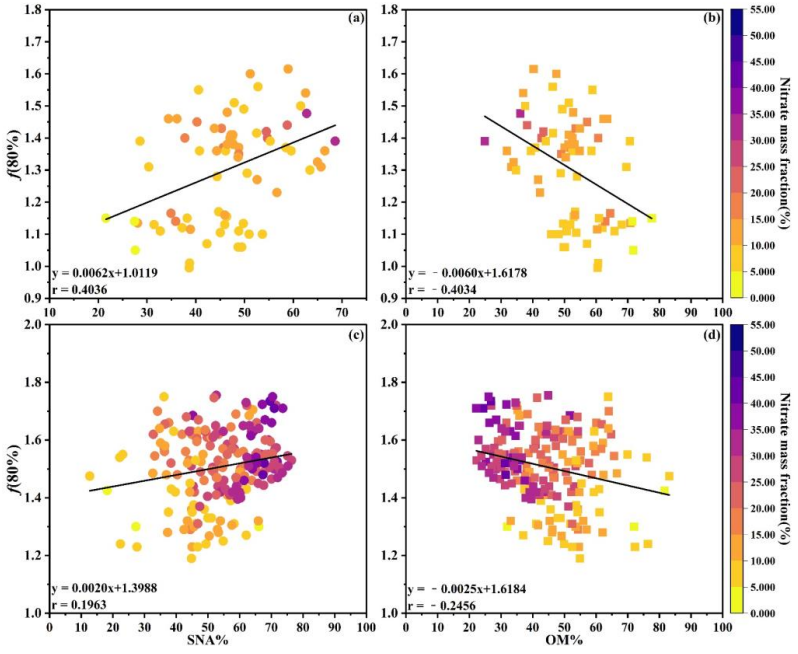

Figure 5. The aerosol scattering hygroscopic growth factor *f*(80%) as a function of SNA and OM mass fraction colored by the nitrate mass fraction. (a) and (b) belong to NPF days; (c) and (d) belong to Non-NPF days. The linear regression function and Pearson's correlation coefficient (R) are given in each panel.

https://doi.org/10.5194/egusphere-2024-2376
Preprint. Discussion started: 18 September 2024

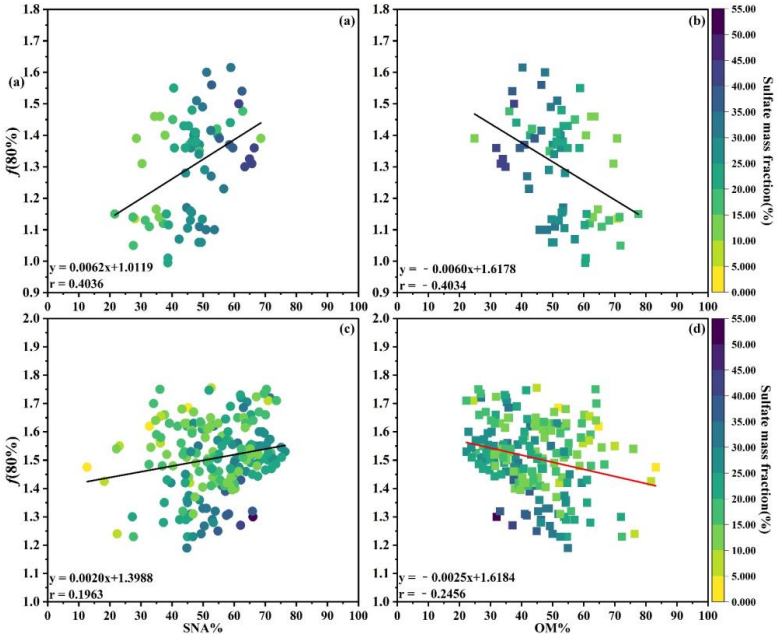

Figure 6. The aerosol scattering hygroscopic growth factor *f*(80%) as a function of SNA and OM mass fraction colored by the sulfate mass fraction. (a) and (b) belong to NPF days; (c) and (d) belong to Non-NPF days. The linear regression function and Pearson's correlation coefficient (R) are given in each panel.

As mentioned above, the aerosol hygroscopic growth was significantly influenced by the proportion of SNA and OM in aerosols. The fitting parameter γ, which depends on the aerosol hygroscopicity, can be employed to characterize the relationship between aerosol hygroscopic growth and SNA. F_o is the relative amount of organic and inorganic matter. γ and F_o were negatively correlated for all scatter plots, and linear regressions of γ versus F_o were fitted (Figure 7). γ and F_O= OM/(OM + NO_3^-) (abbreviated as F_{O+N}, Figure 7a, d) were more strongly correlated than γ and F_O = OM/(OM + SO_4^{2-}) (abbreviated as F_{O+S}, Figure 6b, e). Additionally, the correlation between γ and F_O= OM/(OM + NO_3^- + SO_4^{2-}) (abbreviated as F_{O+N+S}, Figure 6c, f) was observed to be smaller than that of the correlation between γ and F_{O+N}. This is yet more evidence that NO_3^- played more important role than SO_4^{2-} in determining the aerosol hygroscopicity in Xiamen, contrary to the conclusion of Quinn et al. (2005), Malm et al. (2005) and Yan et al. (2009). This findings also underscored the substantial impact of nitrate, aligning with recent research conducted in various regions of China (Zhang et al., 2015;Sun et al., 2020;Liao et al., 2020;Jin et al., 2022).

Over the recent decades, the Chinese government has attached great importance to the air pollution control, and the prominent results have been achieved in reducing SO_2 emissions. As the concentration of SO_2 decreases, there might be an increasing trend

https://doi.org/10.5194/egusphere-2024-2376
Preprint. Discussion started: 18 September 2024

for NH_3 to combine with NO_3^- to form NH_4NO_3, thereby enhancing the role of nitrate in atmospheric processes. The relative low value of f(80%) for NPF days can be explained by the fact that sulfate was the predominant component of the SNA during this period, and was found to be a less effective promoter of the aerosol scattering hygroscopic growth compared to nitrate. During NPF days, there was a stronger correlation between γ and F_{O+S}, while the correlation of γ and F_{O+S} was extremely weak in Non-NPF days, which could be related to the role of sulfuric acid in atmospheric nucleation in NPF days. Li et al. (2021) proposed the parameterization of γ according to its linear relationship beween F and TC, and the R^2 was 0.92, where, F was determined as the mass ratio of F= TC/(TC+ NO_3^- + SO_4^{2-}+ NH_4^+). However, the correlation between γ and F_{O+N+S} in this study was lower than that of Li's report. As the comparison with these parameterizations suggested, the comprehensive chemical composition information was likely in favor of accurate γ parameterizations and subsequent f(RH) determinations.

Overall, SNA are more effective in promoting aerosol hygroscopic growth than that of OM, with nitrate having the strongest impact.

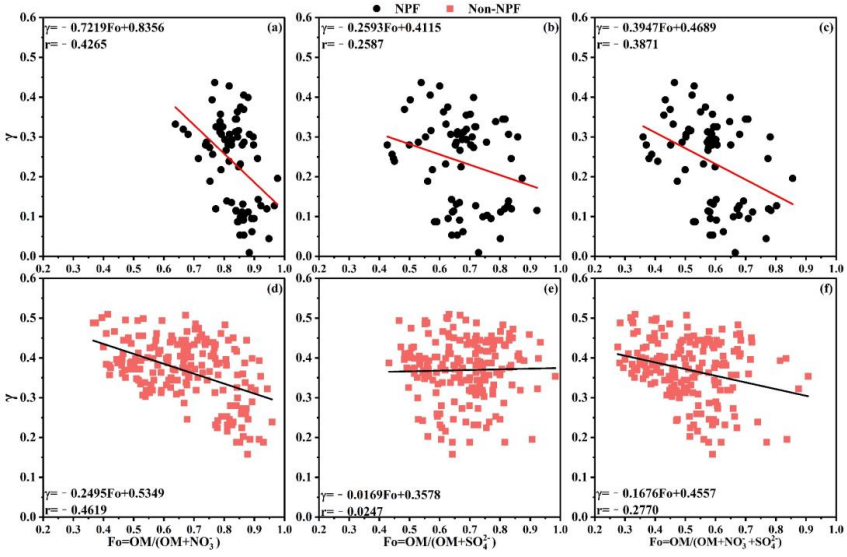

Figure 7. Scatter plots of γ versus the relative amount of OM and inorganics (F_o). (a, d) F_o= OM/(OM+ NO_3^-), (b, e) F_o = OM/(OM + SO_4^{2-}), and (c, f) F_o= OM/(OM+ NO_3^- + SO_4^{2-}). (a), (b) and (c) belong to NPF event; (d), (e) and (f) belong to Non-NPF event. Solid lines represent the linear fit.

3.5 Aerosol hygroscopicity–chemical composition closure

The hygroscopicity parameter κ serves as a highly effective parameter for investigating aerosol hygroscopicity and can be assessed using the humidified nephelometer systems for aerosol light scattering hygroscopic growth factors. The $\kappa_{f(RH)}$, obtained from the measured aerosol scattering hygroscopic growth factor, is a function

https://doi.org/10.5194/egusphere-2024-2376
Preprint. Discussion started: 18 September 2024

of the overall hygroscopicity of aerosol particles (Chen et al., 2014;Kuang et al., 2017;Kuang et al., 2020) and widely used to explain the influence of aerosol hygroscopic growth on aerosol optical properties (Tao et al., 2014;Kuang et al., 2015;Brock et al., 2016). Moreover, κ can be estimated based on the mass concentration and chemical composition of particles, commonly known as κ_{chem}. According to Kuang et al. (2020), $\kappa_{f(RH)}$ accurately represents κ_{chem} and can therefore be used for the aerosol hygroscopicity-chemistry composition closure, which was used to investigate the effect of aerosol chemical composition on the overall aerosol hygroscopicity in this study.

Figure 8 shows the contribution of chemical composition to $\kappa_{f(RH)}$, calculated as the product of κ and its volume fraction for each aerosol chemical composition. During the observation period, the inorganic salts, especially SNA, played a major role in the aerosol hygroscopicity, while some previous studies found that low water-soluble compounds, most likely secondary organic species, predominantly promote new particle formation and have an effect on aerosol hygroscopicity and their cloud condensation nuclei (CCN) activity (Levin et al., 2012;Wu et al., 2015;Väkevä et al., 2002). For aerosol hygroscopicity during NPF days, NH_4HSO_4 (ABS) was the most dominant contributor followed by NH_4NO_3 (AN). Although $(NH_4)_2SO_4$ (AS) ranked third place to aerosol hygroscopicity in NPF, it was still higher than its contributions to Non-NPF days, which was consistent with the mentioned above that sulfate was the main factor influencing the aerosol scattering hygroscopicity growth during NPF period. The donation of AN to aerosol hygroscopicity was predominant during Non-NPF days, while that of AS and ABS decreased substantially compared to those during NPF. The facilitation of organic aerosol (OA) to the aerosol hygroscopicity fluctuated considerably due to variations of OA composition under different events. The 26.57% of $\kappa_{f(RH)}$ attributed to OA in NPF was lower than that in Non-NPF days. This phenomenon was probably associated with the variety of OA components, for instance, secondary organic aerosols (SOAs) exhibiting limited hygroscopicity(Wang et al., 2024). Furthermore, during Non-NPF days, despite the increased contribution of OA to $\kappa_{f(RH)}$, f(RH) was higher than that of NPF days, which might be related to the increase in the overall aerosol hygroscopicity during this period and the change in physical properties of particles during these days (Wu et al., 2016).

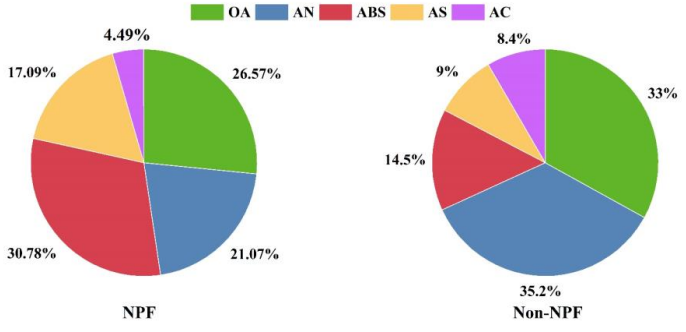

https://doi.org/10.5194/egusphere-2024-2376
Preprint. Discussion started: 18 September 2024

Figure 8. Contribution of aerosol chemical composition to $\kappa_{f(RH)}$ between NPF and Non-NPF days. Green, blue, red, yellow, and purple code reprensent organic aerosol (OA), NH_4NO_3 (AN), NH_4HSO_4 (ABS), $(NH_4)_2SO_4$ (AS), and NH_4Cl (AC), respectively.

Due to the uncertainty in the hygroscopicity of OA, we investigated the characteristics of the hygroscopicity parameter κ_{OA} for organic aerosol, as well as the relationship between κ_{OA} and the oxidative properties of OA (Figure 9). Non-NPF days had the highest value of κ_{OA}, and NPF days had the lowest. The κ_{OA} values were greater than those of the previous study in Beijing (Wu et al., 2016;Kuang et al., 2020;Kuang et al., 2021), but similar to the findings of Chang et al. (2010) at rural site in Ontario, Canada. This could be explained by that the compositions of organic aerosol in Beijing and Xiamen, China, as well as Ontario, Canada were quite different. The discrepantance in κ_{OA} suggests that using a constant κ_{OA} value to calculate κ might lead to a large bias.

To further investigate the factors affecting κ_{OA}, we compared the effect of OA oxidation level on κ_{OA}, where, f_{44} was used to represent the level of OA oxidation. The values of f_{44} in the component mass spectrometry were ratio of m/z 44 to total signals, reflecting the absolute oxidation degree of aerosols. The results showed a slightly weak correlation between κ_{OA} and the oxidation level of OA, indicating that the degree of oxidation was one of significant parameters in determining the hygroscopicity of OA. For both NPF days and Non-NPF days, the hygroscopicity of OA enhanced with its oxidation level. Most of the previous studies on κ_{OA} had shown that the hygroscopicity of OA usually increased with the uplift of oxidation degree of OA, which was also found in this study. Nevertheless, a more pronounced increase in κ_{OA} with elevated f_{44} was observed in Non-NPF days, attributing to the OA components, formation mechanisms, and the species of VOCs among diffenent events, which can also be accounted by the fact that less hygroscopic OA is produced during the NPF process in Xiamen, contrasted with the finding of Liu et al. (2021). Thereby, it could be found that alterations in the component and oxidation of OA might regulate the variation in κ_{OA} (Timonen et al., 2013;Xu et al., 2014;Xu et al., 2017). In addition, the κ_{OA} values in NPF and Non-NPF days were lower than those in the studies of Chen et al. (2017), Liu et al. (2021) and Kuang et al. (2020). These results reflect that the use of parameters related to oxidative properties, such as f_{44} or the ratio of O and C alone is not sufficient to characterize the hygroscopicity of OA, and that the molecular information of OA and the special formation mechanisms should also be considered (Liu et al., 2021). However, OA components is still one of the main driving force of the variation in aerosol hygroscopicity.

https://doi.org/10.5194/egusphere-2024-2376
Preprint. Discussion started: 18 September 2024

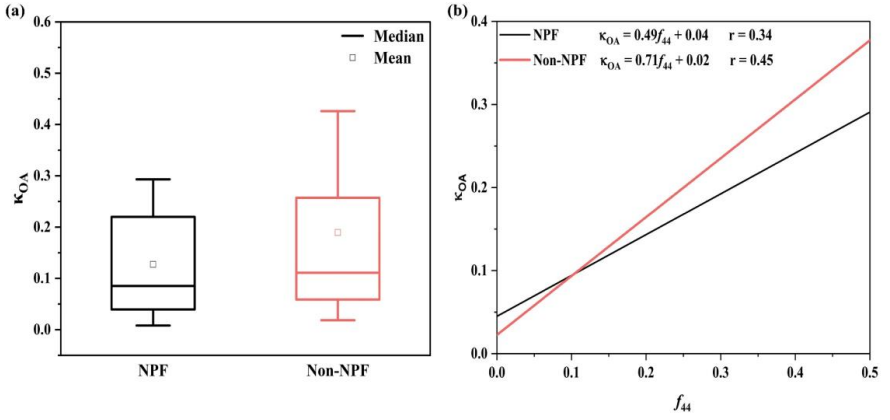

Figure 9. The derived κ_{OA} and f_{44} between NPF and Non-NPF days. (a) Variation of κ_{OA} between NPF and Non-NPF days. (b) The relationship between derived κ_{OA} and f_{44}.

4 Conclusions

In this study, the aerosol scattering hygroscopic growth during the new particle formation in Xiamen, the coastal city of southeast China, was clearly depicted by in situ observations. The distinct aerosol hygroscopic behaviors were evident during NPF events in the urban environment characterized by the elevated ambient temperatures, high levels of relative humidity, and low pollution. The aerosol scattering hygroscopic growth of NPF days was weaker than those of Non-NPF days. However, under high RH conditions (80% to 90%), the f(RH) growth of NPF days exceeded that of Non-NPF days. Furthermore, it was determined that one of the two-parameter fitting equations was more adept at accurately representing the observed f(RH).

The notable variations in f(RH) between NPF and Non-NPF days were impacted by changes in SNA and OM of aerosols. SNA had a more important effect on f(RH) and a higher efficacy in enhancing aerosol hygroscopic growth than that of OM, with nitrate exhibiting the most pronounced impact. Sulfate was highlighted as the dominance in SNA during NPF days, resulting in weaker f(RH) compared to Non-NPF days. The contribution of SNA to aerosol hygroscopicity surpassed that of OM, with ABS and AN dominating in NPF days and Non-NPF days respectively, revealed by the aerosol hygroscopicity–chemical composition closure. The estimated κ_{OA} exhibited a decrease in NPF days compared to Non-NPF days, and it showed an increase corresponding to the level of OA oxidation in both two types of days. The uncertainty in OA hygroscopicity resulted from variations in its components and oxidation states, however it was believed to be an important driver of the alteration in aerosol hygroscopicity. The findings in this study may provide a better explanation of aerosol hygroscopicity properties in the coastal city, which could also offer valuable insights into the use of hygroscopic growth factors in the models of air quality and climate change.

https://doi.org/10.5194/egusphere-2024-2376
Preprint. Discussion started: 18 September 2024

Data availability

The dataset for this paper can be accessed at https://doi.org/10.5281/zenodo.13756825 (Li et al., 2024).

Acknowledgements

This work was funded by the National Natural Science Foundation of China (U22A20578), the Science and Technology Department of Fujian Province (2022L3025), the National Key Research and Development Program (2022YFC3700304), STS Plan Supporting Project of the Chinese Academy of Sciences in Fujian Province (2023T3013), Fujian Provincial Environmental Protection Science & Technology Plan Projects (2023R004), and Xiamen Atmospheric Environment Observation and Research Station of Fujian Province.

Author contributions

ML and JC conceived the conceptual development of the paper. LL made measurements, analyzed the data and wrote the paper. ML designed the project and conducted the field campaigns. ML, XF and JC directed the manuscript development and editing. YC made measurements. All authors contributed to discussion and review.

Competing interests

The authors declare that they have no known competing financial interests or personal relationships that could have appeared to influence the work reported in this paper.

https://doi.org/10.5194/egusphere-2024-2376
Preprint. Discussion started: 18 September 2024

References

Brock, C. A., Wagner, N. L., Anderson, B. E., Attwood, A. R., Beyersdorf, A., Campuzano-Jost, P., Carlton, A. G., Day, D. A., Diskin, G. S., Gordon, T. D., Jimenez, J. L., Lack, D. A., Liao, J., Markovic, M. Z., Middlebrook, A. M., Ng, N. L., Perring, A. E., Richardson, M. S., Schwarz, J. P., Washenfelder, R. A., Welti, A., Xu, L., Ziemba, L. D., and Murphy, D. M.: Aerosol optical properties in the southeastern United States in summer - Part 1: Hygroscopic growth, Atmospheric Chemistry and Physics, 16, 4987-5007, 10.5194/acp-16-4987-2016, 2016.

Carrico, C. M., Kus, P., Rood, M. J., Quinn, P. K., and Bates, T. S.: Mixtures of pollution, dust, sea salt, and volcanic aerosol during ACE-Asia: Radiative properties as a function of relative humidity, Journal of Geophysical Research-Atmospheres, 108, 10.1029/2003jd003405, 2003.

Chang, R. Y. W., Slowik, J. G., Shantz, N. C., Vlasenko, A., Liggio, J., Sjostedt, S. J., Leaitch, W. R., and Abbatt, J. P. D.: The hygroscopicity parameter (κ) of ambient organic aerosol at a field site subject to biogenic and anthropogenic influences: relationship to degree of aerosol oxidation, Atmospheric Chemistry and Physics, 10, 5047-5064, 10.5194/acp-10-5047-2010, 2010.

Charlson, R. J., Schwartz, S. E., Hales, J. M., Cess, R. D., Coakley, J. A., Hansen, J. E., and Hofmann, D. J.: Climate Forcing By Anthropogenic Aerosols, Science, 255, 423-430, 10.1126/science.255.5043.423, 1992.

Chen, G. J., Shi, Q., Xu, L. L., Yu, S. C., Lin, Z. Y., Ji, X. T., Fan, X. L., Hong, Y. W., Li, M. R., Zhang, F. W., Chen, J. F., and Chen, J. S.: Photochemistry in the urban agglomeration along the coastline of southeastern China: Pollution mechanism and control implication, Science of the Total Environment, 901, 10.1016/j.scitotenv.2023.166318, 2023.

Chen, J., Zhao, C. S., Ma, N., and Yan, P.: Aerosol hygroscopicity parameter derived from the light scattering enhancement factor measurements in the North China Plain, Atmospheric Chemistry and Physics, 14, 8105-8118, 10.5194/acp-14-8105-2014, 2014.

Chen, J., Budisulistiorini, S. H., Itoh, M., Lee, W. C., Miyakawa, T., Komazaki, Y., Yang, L. D. Q., and Kuwata, M.: Water uptake by fresh Indonesian peat burning particles is limited by water-soluble organic matter, Atmospheric Chemistry and Physics, 17, 11591-11604, 10.5194/acp-17-11591-2017, 2017.

Chen, L., Zhang, F., Zhang, D. M., Wang, X. M., Song, W., Liu, J. Y., Ren, J. Y., Jiang, S. H., Li, X., and Li, Z. Q.: Measurement report: Hygroscopic growth of ambient fine particles measured at five sites in China, Atmospheric Chemistry and Physics, 22, 6773-6786, 10.5194/acp-22-6773-2022, 2022a.

Chen, T. Z., Chu, B. W., Ma, Q. X., Zhang, P., Liu, J., and He, H.: Effect of relative humidity on SOA formation from aromatic hydrocarbons: Implications from the evolution of gas- and particle -phase species, Science of the Total Environment, 773, 10.1016/j.scitotenv.2021.145015, 2021.

Chen, Y. P., Yang, C., Xu, L. L., Chen, J. S., Zhang, Y. R., Shi, J. Y., Fan, X. L., Zheng, R. H., Hong, Y. W., and Li, M. R.: Chemical composition of NR-PM₁ in

https://doi.org/10.5194/egusphere-2024-2376
Preprint. Discussion started: 18 September 2024

a coastal city of Southeast China: Temporal variations and formation pathways, Atmospheric Environment, 285, 10.1016/j.atmosenv.2022.119243, 2022b.

Covert, D. S., Charlson, R. J., and Ahlquist, N. C.: A Study of the Relationship of Chemical Composition and Humidity to Light Scattering by Aerosols, Journal of Applied Meteorology and Climatology, 11, 968-976, https://doi.org/10.1175/1520-0450(1972)011<0968:ASOTRO>2.0.CO;2, 1972.

Dal Maso, M., Kulmala, M., Riipinen, I., Wagner, R., Hussein, T., Aalto, P. P., and Lehtinen, K. E. J.: Formation and growth of fresh atmospheric aerosols: eight years of aerosol size distribution data from SMEAR II, Hyytiala, Finland, Boreal Environment Research, 10, 323-336, 2005.

Deng, J. J., Zhang, Y. R., Hong, Y. W., Xu, L. L., Chen, Y. T., Du, W. J., and Chen, J. S.: Optical properties of PM2.5 and the impacts of chemical compositions in the coastal city Xiamen in China, Science of the Total Environment, 557, 665-675, 10.1016/j.scitotenv.2016.03.143, 2016.

Ding, J., Zhang, Y., Zheng, N., Zhang, H., Yu, Z., Li, L., Yuan, J., Tang, M., and Feng, Y.: Size Distribution of Aerosol Hygroscopic Growth Factors in Winter in Tianjin, Environmental Science, 42, 574-583, 2021.

Duplissy, J., DeCarlo, P. F., Dommen, J., Alfarra, M. R., Metzger, A., Barmpadimos, I., Prevot, A. S. H., Weingartner, E., Tritscher, T., Gysel, M., Aiken, A. C., Jimenez, J. L., Canagaratna, M. R., Worsnop, D. R., Collins, D. R., Tomlinson, J., and Baltensperger, U.: Relating hygroscopicity and composition of organic aerosol particulate matter, Atmospheric Chemistry and Physics, 11, 1155-1165, 10.5194/acp-11-1155-2011, 2011.

Fierz-Schmidhauser, R., Zieger, P., Vaishya, A., Monahan, C., Bialek, J., O'Dowd, C. D., Jennings, S. G., Baltensperger, U., and Weingartner, E.: Light scattering enhancement factors in the marine boundary layer (Mace Head, Ireland), Journal of Geophysical Research-Atmospheres, 115, 10.1029/2009jd013755, 2010a.

Fierz-Schmidhauser, R., Zieger, P., Wehrle, G., Jefferson, A., Ogren, J. A., Baltensperger, U., and Weingartner, E.: Measurement of relative humidity dependent light scattering of aerosols, Atmospheric Measurement Techniques, 3, 39-50, 10.5194/amt-3-39-2010, 2010b.

Gasso, S., Hegg, D. A., Covert, D. S., Collins, D., Noone, K. J., Ostrom, E., Schmid, B., Russell, P. B., Livingston, J. M., Durkee, P. A., and Jonsson, H.: Influence of humidity on the aerosol scattering coefficient and its effect on the upwelling radiance during ACE-2, Tellus Series B-Chemical and Physical Meteorology, 52, 546-567, 10.1034/j.1600-0889.2000.00055.x, 2000.

Ge, X. L., Zhang, Q., Sun, Y. L., Ruehl, C. R., and Setyan, A.: Effect of aqueous-phase processing on aerosol chemistry and size distributions in Fresno, California, during wintertime, Environmental Chemistry, 9, 221-235, 10.1071/en11168, 2012.

Guan, X., Wang, M., Du, T., Tian, P. F., Zhang, N. Y., Shi, J. S., Chang, Y., Zhang, L., Zhang, M., Song, X., and Sun, Y. J.: Wintertime aerosol optical properties in Lanzhou, Northwest China: Emphasis on the rapid increase of aerosol absorption under high particulate pollution, Atmospheric Environment, 246,

https://doi.org/10.5194/egusphere-2024-2376
Preprint. Discussion started: 18 September 2024

10.1016/j.atmosenv.2020.118081, 2021.
Gysel, M., Crosier, J., Topping, D. O., Whitehead, J. D., Bower, K. N., Cubison, M. J., Williams, P. I., Flynn, M. J., McFiggans, G. B., and Coe, H.: Closure study between chemical composition and hygroscopic growth of aerosol particles during TORCH2, Atmospheric Chemistry and Physics, 7, 6131-6144, 10.5194/acp-7-6131-2007, 2007.
Holmes, N. S.: A review of particle formation events and growth in the atmosphere in the various environments and discussion of mechanistic implications, Atmospheric Environment, 41, 2183-2201, 10.1016/j.atmosenv.2006.10.058, 2007.
IPCC: Climate Change 2021: The Physical Science Basis. Contribution of Working Group I to the Sixth Assessment Report of the Intergovernmental Panel on Climate Change, Cambridge University Press, In Press, 2021.
Jin, X. A., Li, Z. Q., Wu, T., Wang, Y. Y., Su, T. N., Ren, R. M., Wu, H., Zhang, D. M., Li, S. Z., and Cribb, M.: Differentiating the Contributions of Particle Concentration, Humidity, and Hygroscopicity to Aerosol Light Scattering at Three Sites in China, Journal of Geophysical Research-Atmospheres, 127, 10.1029/2022jd036891, 2022.
Kalkavouras, P., BougiatiotI, A., Hussein, T., Kalivitis, N., Stavroulas, I., Michalopoulos, P., and Mihalopoulos, N.: Regional New Particle Formation over the Eastern Mediterranean and Middle East, Atmosphere, 12, 10.3390/atmos12010013, 2021.
Kotchenruther, R. A., and Hobbs, P. V.: Humidification factors of aerosols from biomass burning in Brazil, Journal of Geophysical Research-Atmospheres, 103, 32081-32089, 10.1029/98jd00340, 1998.
Kotchenruther, R. A., Hobbs, P. V., and Hegg, D. A.: Humidification factors for atmospheric aerosols off the mid-Atlantic coast of the United States, Journal of Geophysical Research-Atmospheres, 104, 2239-2251, 10.1029/98jd01751, 1999.
Kuang, Y., Zhao, C. S., Tao, J. C., and Ma, N.: Diurnal variations of aerosol optical properties in the North China Plain and their influences on the estimates of direct aerosol radiative effect, Atmospheric Chemistry and Physics, 15, 5761-5772, 10.5194/acp-15-5761-2015, 2015.
Kuang, Y., Zhao, C. S., Tao, J. C., Bian, Y. X., Ma, N., and Zhao, G.: A novel method for deriving the aerosol hygroscopicity parameter based only on measurements from a humidified nephelometer system, Atmospheric Chemistry and Physics, 17, 6651-6662, 10.5194/acp-17-6651-2017, 2017.
Kuang, Y., He, Y., Xu, W. Y., Zhao, P. S., Cheng, Y. F., Zhao, G., Tao, J. C., Ma, N., Su, H., Zhang, Y. Y., Sun, J. Y., Cheng, P., Yang, W. D., Zhang, S. B., Wu, C., Sun, Y. L., and Zhao, C. S.: Distinct diurnal variation in organic aerosol hygroscopicity and its relationship with oxygenated organic aerosol, Atmospheric Chemistry and Physics, 20, 865-880, 10.5194/acp-20-865-2020, 2020.
Kuang, Y., Huang, S., Xue, B. A., Luo, B. A., Song, Q. C., Chen, W., Hu, W. W., Li, W., Zhao, P. S., Cai, M. F., Peng, Y. W., Qi, J. P., Li, T. G., Wang, S. H., Chen, D. H., Yue, D. L., Yuan, B., and Shao, M.: Contrasting effects of secondary organic aerosol formations on organic aerosol hygroscopicity, Atmospheric Chemistry and Physics, 21,

https://doi.org/10.5194/egusphere-2024-2376
Preprint. Discussion started: 18 September 2024

10375-10391, 10.5194/acp-21-10375-2021, 2021.
Kulmala, M., Petaja, T., Nieminen, T., Sipila, M., Manninen, H. E., Lehtipalo, K., Dal Maso, M., Aalto, P. P., Junninen, H., Paasonen, P., Riipinen, I., Lehtinen, K. E. J., Laaksonen, A., and Kerminen, V. M.: Measurement of the nucleation of atmospheric aerosol particles, Nature Protocols, 7, 1651-1667, 10.1038/nprot.2012.091, 2012.
Levin, E. J. T., Prenni, A. J., Petters, M. D., Kreidenweis, S. M., Sullivan, R. C., Atwood, S. A., Ortega, J., DeMott, P. J., and Smith, J. N.: An annual cycle of size-resolved aerosol hygroscopicity at a forested site in Colorado, Journal of Geophysical Research-Atmospheres, 117, 10.1029/2011jd016854, 2012.
Li, J. W., Zhang, Z. S., Wu, Y. F., Tao, J., Xia, Y. J., Wang, C. Y., and Zhang, R. J.: Effects of chemical compositions in fine particles and their identified sources on hygroscopic growth factor during dry season in urban Guangzhou of South China, Science of the Total Environment, 801, 10.1016/j.scitotenv.2021.149749, 2021.
Liao, W. J., Zhou, J. B., Zhu, S. J., Xiao, A. S., Li, K., and Schauer, J. J.: Characterization of aerosol chemical composition and the reconstruction of light extinction coefficients during winter in Wuhan, China, Chemosphere, 241, 10.1016/j.chemosphere.2019.125033, 2020.
Liu, H., and Zhao, C.: Design of a Humidified Nephelometer System with High Time Resolution, Acta Scientiarum Naturalium Universitatis Pekinensis, 52, 999-1004, 2016.
Liu, H. J., Zhao, C. S., Nekat, B., Ma, N., Wiedensohler, A., van Pinxteren, D., Spindler, G., Muller, K., and Herrmann, H.: Aerosol hygroscopicity derived from size-segregated chemical composition and its parameterization in the North China Plain, Atmospheric Chemistry and Physics, 14, 2525-2539, 10.5194/acp-14-2525-2014, 2014.
Liu, J. Y., Ren, C. H., Huang, X., Nie, W., Wang, J. P., Sun, P., Chi, X. G., and Ding, A. J.: Increased Aerosol Extinction Efficiency Hinders Visibility Improvement in Eastern China, Geophysical Research Letters, 47, 10.1029/2020gl090167, 2020a.
Liu, J. Y., Zhang, F., Xu, W. Q., Sun, Y. L., Chen, L., Li, S. Z., Ren, J. Y., Hu, B., Wu, H., and Zhang, R. Y.: Hygroscopicity of Organic Aerosols Linked to Formation Mechanisms, Geophysical Research Letters, 48, 10.1029/2020gl091683, 2021.
Liu, T. T., Hu, B. Y., Yang, Y. X., Li, M. R., Hong, Y. W., Xu, X. B., Xu, L. L., Chen, N. H., Chen, Y. T., Xiao, H., and Chen, J. S.: Characteristics and source apportionment of PM2.5 on an island in Southeast China: Impact of sea-salt and monsoon, Atmospheric Research, 235, 10.1016/j.atmosres.2019.104786, 2020b.
Liu, T. T., Hong, Y. W., Li, M. R., Xu, L. L., Chen, J. S., Bian, Y. H., Yang, C., Dan, Y. B., Zhang, Y. N., Xue, L. K., Zhao, M., Huang, Z., and Wang, H.: Atmospheric oxidation capacity and ozone pollution mechanism in a coastal city of southeastern China: analysis of a typical photochemical episode by an observation-based model, Atmospheric Chemistry and Physics, 22, 2173-2190, 10.5194/acp-22-2173-2022, 2022.
Liu, X. G., Zhang, Y. H., Cheng, Y. F., Hu, M., and Han, T. T.: Aerosol hygroscopicity and its impact on atmospheric visibility and radiative forcing in Guangzhou during the 2006 PRIDE-PRD campaign, Atmospheric Environment, 60, 59-67, 10.1016/j.atmosenv.2012.06.016, 2012.

https://doi.org/10.5194/egusphere-2024-2376
Preprint. Discussion started: 18 September 2024

739 Malm, W. C., and Day, D. E.: Estimates of aerosol species scattering characteristics as
740 a function of relative humidity, Atmospheric Environment, 35, 2845-2860,
741 10.1016/s1352-2310(01)00077-2, 2001.
742 Malm, W. C., Day, D. E., Kreidenweis, S. M., Collett, J. L., Carrico, C., McMeeking,
743 G., and Lee, T.: Hygroscopic properties of an organic-laden aerosol, Atmospheric
744 Environment, 39, 4969-4982, 10.1016/j.atmosenv.2005.05.014, 2005.
745 Pan, X. L., Yan, P., Tang, J., Ma, J. Z., Wang, Z. F., Gbaguidi, A., and Sun, Y. L.:
746 Observational study of influence of aerosol hygroscopic growth on scattering
747 coefficient over rural area near Beijing mega-city, Atmospheric Chemistry and Physics,
748 9, 7519-7530, 10.5194/acp-9-7519-2009, 2009.
749 Petters, M. D., and Kreidenweis, S. M.: A single parameter representation of
750 hygroscopic growth and cloud condensation nucleus activity, Atmospheric Chemistry
751 and Physics, 7, 1961-1971, 10.5194/acp-7-1961-2007, 2007.
752 Quinn, P. K., Bates, T. S., Baynard, T., Clarke, A. D., Onasch, T. B., Wang, W., Rood,
753 M. J., Andrews, E., Allan, J., Carrico, C. M., Coffman, D., and Worsnop, D.: Impact of
754 particulate organic matter on the relative humidity dependence of light scattering: A
755 simplified parameterization, Geophysical Research Letters, 32, 10.1029/2005gl024322,
756 2005.
757 Ren, R. M., Li, Z. Q., Yan, P., Wang, Y. Y., Wu, H., Cribb, M., Wang, W., Jin, X. A., Li,
758 Y. A., and Zhang, D. M.: Measurement report: The effect of aerosol chemical
759 composition on light scattering due to the hygroscopic swelling effect, Atmospheric
760 Chemistry and Physics, 21, 9977-9994, 10.5194/acp-21-9977-2021, 2021.
761 Shen, X. J., Sun, J. Y., Ma, Q. L., Zhang, Y. M., Zhong, J. T., Yue, Y., Xia, C., Hu, X.
762 Y., Zhang, S. N., and Zhang, X. Y.: Long-term trend of new particle formation events
763 in the Yangtze River Delta, China and its influencing factors: 7-year dataset analysis,
764 Science of the Total Environment, 807, 10.1016/j.scitotenv.2021.150783, 2022.
765 Sheridan, P. J., Delene, D. J., and Ogren, J. A.: Four years of continuous surface aerosol
766 measurements from the Department of Energy's Atmospheric Radiation Measurement
767 Program Southern Great Plains Cloud and Radiation Testbed site, Journal of
768 Geophysical Research-Atmospheres, 106, 20735-20747, 10.1029/2001jd000785, 2001.
769 Sheridan, P. J., Jefferson, A., and Ogren, J. A.: Spatial variability of submicrometer
770 aerosol radiative properties over the Indian Ocean during INDOEX, Journal of
771 Geophysical Research-Atmospheres, 107, 10.1029/2000jd000166, 2002.
772 Sipilä, M., Berndt, T., Petäjä, T., Brus, D., Vanhanen, J., Stratmann, F., Patokoski, J.,
773 Mauldin, R. L., Hyvärinen, A. P., Lihavainen, H., and Kulmala, M.: The Role of
774 Sulfuric Acid in Atmospheric Nucleation, Science, 327, 1243-1246,
775 10.1126/science.1180315, 2010.
776 Sun, P., Nie, W., Wang, T. Y., Chi, X. G., Huang, X., Xu, Z., Zhu, C. J., Wang, L., Qi,
777 X. M., Zhang, Q., and Ding, A. J.: Impact of air transport and secondary formation on
778 haze pollution in the Yangtze River Delta: In situ online observations in Shanghai and
779 Nanjing, Atmospheric Environment, 225, 10.1016/j.atmosenv.2020.117350, 2020.
780 Sun, Y. L., Wang, Z. F., Fu, P. Q., Jiang, Q., Yang, T., Li, J., and Ge, X. L.: The impact

https://doi.org/10.5194/egusphere-2024-2376
Preprint. Discussion started: 18 September 2024

of relative humidity on aerosol composition and evolution processes during wintertime in Beijing, China, Atmospheric Environment, 77, 927-934, 10.1016/j.atmosenv.2013.06.019, 2013.

Tang, I. N.: Chemical and size effects of hygroscopic aerosols on light scattering coefficients, Journal of Geophysical Research-Atmospheres, 101, 19245-19250, 10.1029/96jd03003, 1996.

Tao, J. C., Zhao, C. S., Ma, N., and Liu, P. F.: The impact of aerosol hygroscopic growth on the single-scattering albedo and its application on the NO₂ photolysis rate coefficient, Atmospheric Chemistry and Physics, 14, 12055-12067, 10.5194/acp-14-12055-2014, 2014.

Timonen, H., Carbone, S., Aurela, M., Saarnio, K., Saarikoski, S., Ng, N. L., Canagaratna, M. R., Kulmala, M., Kerminen, V. M., Worsnop, D. R., and Hillamo, R.: Characteristics, sources and water-solubility of ambient submicron organic aerosol in springtime in Helsinki, Finland, Journal of Aerosol Science, 56, 61-77, 10.1016/j.jaerosci.2012.06.005, 2013.

Titos, G., Lyamani, H., Cazorla, A., Sorribas, M., Foyo-Moreno, I., Wiedensohler, A., and Alados-Arboledas, L.: Study of the relative humidity dependence of aerosol light-scattering in southern Spain, Tellus Series B-Chemical and Physical Meteorology, 66, 10.3402/tellusb.v66.24536, 2014.

Väkevä, M., Hämeri, K., and Aalto, P. P.: Hygroscopic properties of nucleation mode and Aitken mode particles during nucleation bursts and in background air -: art. no. 8104, Journal of Geophysical Research-Atmospheres, 107, 10.1029/2000jd000176, 2002.

Wang, J., Li, M., Li, L., Zheng, R., Fan, X., Hong, Y., Xu, L., Chen, J., and Hu, B.: Particle number size distribution and new particle formation in Xiamen, the coastal city of Southeast China in wintertime, The Science of the total environment, 826, 154208, 10.1016/j.scitotenv.2022.154208, 2022.

Wang, M. L., Chen, Y. Q., Fu, H. Y., Qu, X. L., Shen, G. F., Li, B. G., and Zhu, D. Q.: Combined analyses of hygroscopic properties of organic and inorganic components of three representative black carbon samples recovered from pyrolysis, Science of the Total Environment, 771, 10.1016/j.scitotenv.2021.145393, 2021.

Wang, Y., Li, J., Fang, F., Zhang, P., He, J., Pöhlker, M. L., Henning, S., Tang, C., Jia, H., Wang, Y., Jian, B., Shi, J., and Huang, J.: In-situ observations reveal weak hygroscopicity in the Southern Tibetan Plateau: implications for aerosol activation and indirect effects, npj Climate and Atmospheric Science, 7, 77, 10.1038/s41612-024-00629-x, 2024.

Won, W. S., Oh, R., Lee, W., Ku, S., Su, P. C., and Yoon, Y. J.: Hygroscopic properties of particulate matter and effects of their interactions with weather on visibility, Scientific Reports, 11, 10.1038/s41598-021-95834-6, 2021.

Wu, Y. F., Wang, X. J., Yan, P., Zhang, L. M., Tao, J., Liu, X. Y., Tian, P., Han, Z. W., and Zhang, R. J.: Investigation of hygroscopic growth effect on aerosol scattering coefficient at a rural site in the southern North China Plain, Science of the Total

https://doi.org/10.5194/egusphere-2024-2376
Preprint. Discussion started: 18 September 2024

Environment, 599, 76-84, 10.1016/j.scitotenv.2017.04.194, 2017.
Wu, Z. J., Poulain, L., Birmili, W., Gröss, J., Niedermeier, N., Wang, Z. B., Herrmann, H., and Wiedensohler, A.: Some insights into the condensing vapors driving new particle growth to CCN sizes on the basis of hygroscopicity measurements, Atmospheric Chemistry and Physics, 15, 13071-13083, 10.5194/acp-15-13071-2015, 2015.
Wu, Z. J., Zheng, J., Shang, D. J., Du, Z. F., Wu, Y. S., Zeng, L. M., Wiedensohler, A., and Hu, M.: Particle hygroscopicity and its link to chemical composition in the urban atmosphere of Beijing, China, during summertime, Atmospheric Chemistry and Physics, 16, 1123-1138, 10.5194/acp-16-1123-2016, 2016.
Wu, Z. J., Wang, Y., Tan, T. Y., Zhu, Y. S., Li, M. R., Shang, D. J., Wang, H. C., Lu, K. D., Guo, S., Zeng, L. M., and Zhang, Y. H.: Aerosol Liquid Water Driven by Anthropogenic Inorganic Salts: Implying Its Key Role in Haze Formation over the North China Plain, Environmental Science & Technology Letters, 5, 160-166, 10.1021/acs.estlett.8b00021, 2018.
Xia, C., Sun, J. Y., Qi, X. F., Shen, X. J., Zhong, J. T., Zhang, X. Y., Wang, Y. Q., Zhang, Y. M., and Hu, X. Y.: Observational study of aerosol hygroscopic growth on scattering coefficient in Beijing: A case study in March of 2018, Science of the Total Environment, 685, 239-247, 10.1016/j.scitotenv.2019.05.283, 2019.
Xia, C., Sun, J. Y., Hu, X. Y., Shen, X. J., Zhang, Y. M., Zhang, S. A., Wang, J. L., Liu, Q., Lu, J. Y., Liu, S., and Zhang, X. Y.: Effects of hygroscopicity on aerosol optical properties and direct radiative forcing in Beijing: Based on two-year observations, Science of the Total Environment, 857, 10.1016/j.scitotenv.2022.159233, 2023.
Xu, W., Guo, S., Gomez-Hernandez, M., Zamora, M. L., Secrest, J., Marrero-Ortiz, W., Zhang, A. L., Collins, D. R., and Zhang, R. Y.: Cloud forming potential of oligomers relevant to secondary organic aerosols, Geophysical Research Letters, 41, 6538-6545, 10.1002/2014gl061040, 2014.
Xu, W. Q., Han, T. T., Du, W., Wang, Q. Q., Chen, C., Zhao, J., Zhang, Y. J., Li, J., Fu, P. Q., Wang, Z. F., Worsnop, D. R., and Sun, Y. L.: Effects of Aqueous-Phase and Photochemical Processing on Secondary Organic Aerosol Formation and Evolution in Beijing, China, Environmental Science & Technology, 51, 762-770, 10.1021/acs.est.6b04498, 2017.
Yan, P., Pan, X. L., Tang, J., Zhou, X. J., Zhang, R. J., and Zeng, L. M.: Hygroscopic growth of aerosol scattering coefficient: A comparative analysis between urban and suburban sites at winter in Beijing, Particuology, 7, 52-60, 10.1016/j.partic.2008.11.009, 2009.
Yu, Y. L., Zhao, C. S., Kuang, Y., Tao, J. C., Zhao, G., Shen, C. Y., and Xu, W. Y.: A parameterization for the light scattering enhancement factor with aerosol chemical compositions, Atmospheric Environment, 191, 370-377, 10.1016/j.atmosenv.2018.08.016, 2018.
Zhang, L., Sun, J. Y., Shen, X. J., Zhang, Y. M., Che, H., Ma, Q. L., Zhang, Y. W., Zhang, X. Y., and Ogren, J. A.: Observations of relative humidity effects on aerosol light

https://doi.org/10.5194/egusphere-2024-2376
Preprint. Discussion started: 18 September 2024

scattering in the Yangtze River Delta of China, Atmospheric Chemistry and Physics, 15, 8439-8454, 10.5194/acp-15-8439-2015, 2015.

Zhao, P. S., Ding, J., Du, X., and Su, J.: High time-resolution measurement of light scattering hygroscopic growth factor in Beijing: A novel method for high relative humidity conditions, Atmospheric Environment, 215, 10.1016/j.atmosenv.2019.116912, 2019.

Zhou, S. Z., Wu, L. L., Guo, J. C., Chen, W. H., Wang, X. M., Zhao, J., Cheng, Y. F., Huang, Z. Z., Zhang, J. P., Sun, Y. L., Fu, P. Q., Jia, S. G., Tao, J., Chen, Y. N., and Kuang, J. X.: Measurement report: Vertical distribution of atmospheric particulate matter within the urban boundary layer in southern China - size-segregated chemical composition and secondary formation through cloud processing and heterogeneous reactions, Atmospheric Chemistry and Physics, 20, 6435-6453, 10.5194/acp-20-6435-2020, 2020.

Zieger, P., Fierz-Schmidhauser, R., Gysel, M., Strom, J., Henne, S., Yttri, K. E., Baltensperger, U., and Weingartner, E.: Effects of relative humidity on aerosol light scattering in the Arctic, Atmospheric Chemistry and Physics, 10, 3875-3890, 10.5194/acp-10-3875-2010, 2010.

Zieger, P., Fierz-Schmidhauser, R., Poulain, L., Muller, T., Birmili, W., Spindler, G., Wiedensohler, A., Baltensperger, U., and Weingartner, E.: Influence of water uptake on the aerosol particle light scattering coefficients of the Central European aerosol, Tellus Series B-Chemical and Physical Meteorology, 66, 10.3402/tellusb.v66.22716, 2014.